

Bond Graph Model-Based Methods for Fault Diagnosis: A Comparative Study

Yacine Lounici^{1*}, Youcef Touati¹, Smail Adjerid¹

¹ Solid Mechanics and Systems Laboratory, Department of Mechanical Engineering, Faculty of Engineering Sciences, M'hmed Bougara University, Boumerdes 35000, Algeria.
E-mails: y.lounici@univ-boumerdes.dz, youcef.touati@polytech-lille.fr, adjesmail@yahoo.fr

Abstract—Advanced methods of fault diagnosis become increasingly significant for improving the safety, reliability and efficiency of dynamic systems in various domains of industrial engineering. This paper reviews and compares three bond graph model-based methods for fault diagnosis. These methods are causality inversion method, augmented Analytical redundancy relation method, and fault estimation method. These methods are applied to a simulation model of an electrical system. This latter is used to simulate the system variables in both normal and faulty situations and to generate residuals for fault detection and isolation. The results of the case study are compared for highlighting the fault diagnosis performance and capability of a method over another. The result shows that the fault estimation method has a better diagnosis performance when compared to the other methods.

Keywords—*Diagnosis, Bond graph, Causality inversion, Augmented Analytical redundancy relation, Fault estimation.*

I. INTRODUCTION

Nowadays, the growing demand for safety, reliability, and efficiency of modern industrial systems motivates the development of new fault diagnosis methods for the decision support system. These methods are usually employed for avoiding critical situations that may due to the propagation of the faults, which affect the system dynamics. The fault diagnosis is performed by two steps: alarm generation (Fault detection FD), and the identification of 'the faulty component Fault isolation (I). Via FDI procedures, an alarm can be created if the fault occurs. However, the magnitude of the fault cannot be obtained by these procedures. The magnitude of the fault is obtained using another procedure named fault estimation (FE).

In the last decade, several approaches have emerged allowing to design and implement the fault detection and isolation (FDI) procedures using the so-called qualitative and quantitative approaches [1]. The qualitative approach is essentially based on artificial intelligence or recognition forms developed in [2]. This approach consists of distributing the parametric space in different classes corresponding to known modes of operation based on prior knowledge of the system (model-free). Among the pattern recognition methods used for diagnosis, the principal component analysis (PCA) [3, 4] is used which all operation modes (normal and failing) must be known in advance, which often unrealizable in real systems. In order to perform a reliable diagnosis, model-free methods

such as AI-based require data of all the possible faulty component which is very expansive and exhausting.

The quantitative approaches are mostly based on state space and input-output models and are more related to the model-based methods. Some of them use the observer [5, 6] to generate (residuals (r)) a difference between the measured output and the reference expected behavior of the system. In this context, the parity space method [7, 8] consists of eliminating all the system states in which all system elements are known. Compared to the aforementioned approaches, the BG approach can be an alternative solution for dealing with both sensor, actuator and parameter faults.

The FDI using BG approach is based on the generation of analytical redundancy relations (ARRs). Moreover, the residuals represent the numerical evaluation of these ARRs and are used for real-time diagnosis. The residuals should converge to zero in normal operation, while in a faulty situation the residuals exceed certain values named the thresholds. In addition, the causal and structural properties of the BG model are used to eliminate systematically the unknown variables using a covering causal paths methodology [9]. In the BG approach, the fault isolation is performed through the Boolean fault signature matrix (FSM). This matrix is built using the binary sensitivity of the ARRs. Thus, the comparison between all fault signatures allows the knowledge of the faulty components that can be detected and isolated [10].

In the present work, we compare three methods that intend to improve the fault diagnosis procedure using the BG approach. The first is the causality inversion method. The latter is based on the generation of ARRs from the BG model in preferred derivative causality, where the number of ARRs that can be obtained is equal to the number of junctions having at least an associated detector, plus the number of redundant detectors. These ARRs can then be used to build the FSM in order to isolate the faults. The second is the augmented Analytical redundancy relations method. This method allows the generation of different versions of the same ARR from each observed junction so that additional non-redundant ARRs can be obtained. The third method is based on the sensitivity relation between the residuals and the faults to generate the fault estimation equations. The comparison between the two estimations of each fault is an additional residual.

The rest of this paper is organized as follows: Section 2 details the causality inversion method for *ARRs* generation and FSM. The augmented Analytical redundancy relations method and fault estimation method are described in Section 3, and 4 respectively. Application with simulation results and comparative analysis are presented in Section 5. Finally, the conclusions are given in Section 6.

II. CAUSALITY INVERSION METHOD AND FDI

A bond graph (BG) is a multidisciplinary graphical modeling language based on energy transfer phenomena. The energy exchange link, called power bond with two generic power variables named flow f and effort e , associated with every bond, where $e \times f = \text{power}$ (Fig. 1). The set of possible BG elements is:

$$S = \{R \cup C \cup I \cup TF \cup GY \cup Se \cup Sf \cup De \cup Df \cup J\}$$

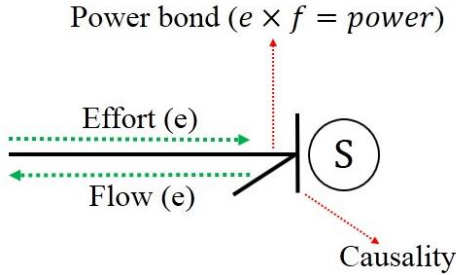


Fig. 1. Bond Graph representation.

The set of elements $\{R, C, I\}$ models the system parameters where R , C , and I are the dissipation element, capacitance element, and inertial element respectively. The latter along with the elements $\{GY, TF, 0, 1\}$ define the global structure of the system where GY and TF are the gyrator element and transformer element respectively. Sensors are represented by effort (Se), and flow (Sf) detectors. Junction 1 (or 0) implies that all the connected bonds have the same flow (or effort) and the sum of efforts (or flows) equals zero. (Sf) and (Se) are the sources of flow and effort, respectively. For more information about BG modeling, see [11].

A. *ARRs* generation using the causality inversion method

The FDI using BG approach is based on the generation of *ARRs*. The latter represents the physical constraints calculated from an observable and over-constrained subsystem and they have the form: $h(K) = 0$ for any function h and set of known variables K . Evaluation of an *ARR* yields a residual (r): $r[h(K)]$. In order to obtain the *ARRs* in a systematic manner, Ould Bouamama et al. [12] introduced the causality inversion method.

Definition 1. Inversion of detectors, this means that the flow (Df) (or effort (De)) detector used for modeling (Fig. 2a) becomes (SSf) (or SSe) (Fig. 2b) and imposes the flow (or

effort) to the 1 (or 0) junction connected to this detector used for diagnosis respectively [14].

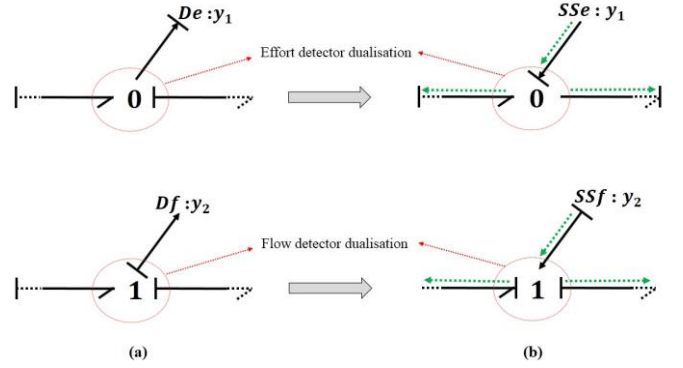


Fig. 2. Inversion of detectors.

The following steps are taken to generate *ARRs* using the causality inversion method:

Step 1: Obtain the BG model of the system in derivative causality, by inverting detectors when possible. Thus, the BG model of diagnosis is obtained.

Step 2: From the BG model, an *ARR* is obtained from each observed junction by writing its junction equation and eliminating the unknown variables by using the causal path propagation.

Step 3: For any non-dualized detector, a material redundancy is presented in the system. The latter exists if there are causal paths from one or more detectors in inverted causality to the non-inverted one, without passing through any two-port or passive element [13].

B. Fault isolation using fault signature matrix

The fault isolation can be done using the FSM that can be directly deduced either from the *ARRs* or from the BG model. In the FSM, the Boolean relations ($S_{i,j} \in \{0,1\}$) between the residuals and the parameters are represented, as illustrated in Table 1. Where the rows are the parameters that represent the components ($C_{i,j} = 1, 2, \dots, m$) and the columns are the residuals ($r_{i,j} = 1, 2, \dots, n$).

TABLE I. FAULT SIGNATURE MATRIX

	r_1	r_2	\dots	r_n	Db_m	Ib_m
C_1	$S_{1,1}$	$S_{1,2}$	\dots	$S_{1,n}$	Db_1	Ib_1
C_2	$S_{2,1}$	$S_{2,2}$	\dots	$S_{2,n}$	Db_2	Ib_2
C_m	$S_{m,1}$	$S_{m,2}$	\dots	$S_{m,n}$	Db_m	Ib_m

Let us define $S^{m \times n}$ as a matrix of Boolean values $S_{i,j}$, where:

$S_{i,j} = \{1 \text{ When } j^{\text{th}} \text{ } ARR(r_j) \text{ contains the parameter of the } i^{\text{th}} \text{ component.}$

$S_{i,j} = \{0 \text{ Otherwise.}$

Let us define G (column I_b) as an isolability vector, where:

$$g_i = \begin{cases} 1 & \text{When the signature is unique.} \\ 0 & \text{Otherwise.} \end{cases}$$

III. AUGMENTED ANALYTICAL REDUNDANCY RELATION METHOD

In [12, 13], it was shown that the number of *ARRs* which can be obtained by the causality inversion method is equal to the number of junctions having at least an associated detector. However, this last statement is not always valid. The causality inversion method only finds part of the possible solution set, because this method does not exploit all possible sensor combinations. Moreover, if sensor combinations are performed, augmented *ARRs* can be obtained [14]. These combinations can improve the diagnosis procedure, and consequently increase the number of the isolable faults.

Let us use an illustrative example to explain the above method. Fig. 3a shows a BG model in derivative causality used for diagnosis, where the two detectors have been dualized to corresponding sources of information ($De: y_1 \rightarrow SSe: y_1$) and ($Df: y_2 \rightarrow SSf: y_2$). By applying the causality inversion method, two *ARRs* can be obtained:

$$ARR_1 = f_1(y_1, y_2, I_0, \dots) = 0 \quad (1)$$

$$ARR_2 = f_1(y_1, y_2, \dots) = 0 \quad (2)$$

However, consider that the source of the signal $SSe: y_1$ is disregarded, and only $SSf: y_2$ is used for diagnosis as depicted in Fig.3b. In this case, an augmented *ARR* of the following form can be obtained:

$$ARR_3 = f_3(y_2, I_0, \dots) = 0 \quad (3)$$

Following the same procedure while using the information from the signal source $SSe: y_1$, and ignoring the one of $SSf: y_2$, another augmented *ARR* can be generated:

$$ARR_4 = f_4(y_1, I_0, \dots) = 0 \quad (4)$$

Nevertheless, these combinations do not allow generating the extra *ARRs* from the covering path procedure. Therefore, the bicausality notion is proposed, which is introduced in [15].

IV. FAULT ESTIMATION METHOD

If faults have the same signature and two sensitive residuals, they can be isolated if the sensitivity relations between the faults and the residuals are different [16]. As an example, let us consider two faults (F_1, F_2) and two residuals (r_1, r_2) where:

- Γ_{F_1, r_1} is the sensitivity relation between F_1 and r_1 .

- Γ_{F_1, r_2} is the sensitivity relation between F_1 and r_2 .
- Γ_{F_2, r_1} is the sensitivity relation between F_2 and r_1 .
- Γ_{F_2, r_2} is the sensitivity relation between F_2 and r_2 .

As reported by [17], the faults can be estimated from a sensitive residual by using the sensitivity relation. So, each fault (F_1 or F_2) can be estimated from r_1 and r_2 . The comparison between the two estimations of each fault is residual. The latter is not sensitive to the estimated fault. Using the procedure illustrated in Fig. 4, the following equations can be generated:

$$\begin{cases} (a) : F_1 = \Gamma_{F_1, r_1}(r_1) \\ (b) : F_1 = \Gamma_{F_1, r_2}(r_2) \\ (c) : F_2 = \Gamma_{F_2, r_1}(r_1) \\ (d) : F_2 = \Gamma_{F_2, r_2}(r_2) \end{cases} \quad (5)$$

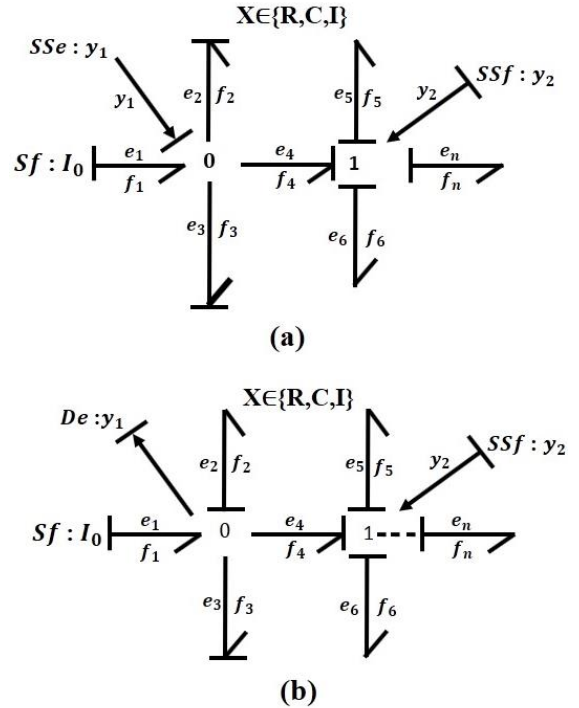


Fig. 3. BG model in preferred derivative causality, (a) Both $SSe: y_1$ and $SSf: y_2$ are dualized, and (b) Without dualizing $De: y_1$.

We remark that the fault F_1 is calculated with two ways, and using two estimation equations (Eq. 5a and Eq. 5b). This fault is isolated if the two results of these two estimation equations are equal, and in the same time, the two estimation equations of the second fault F_2 (Eq. 5c and Eq. 5d) are not equal.

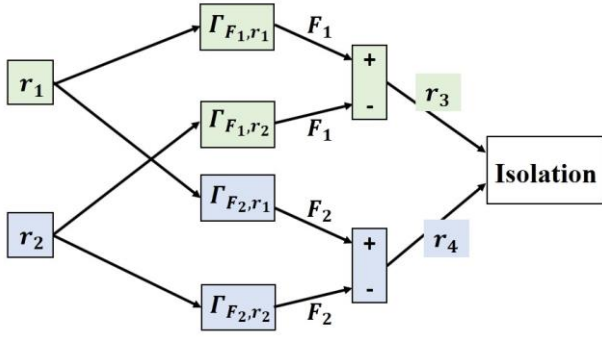


Fig. 4. Fault isolation using sensitivity relations.

The sensitivity relations are obtained from the BG model using the following rules:

- Model the fault by replacing the BG element by its BG linear fractional transformation (BG-LFT) element [18], Where the modulated source MSf (or MSe) represents the flow (or effort) generated by the fault.
- Apply the bi-causality on the modulated source and the sensor associated with a residual in order to eliminate the unknown variables appearing in the expression of the sensitivity relation.
- Use the causal and the structural proprieties of the BG to generate the sensitivity relation between the residual and the fault.

Let us explain the above rules through an illustrative example (Fig. 5a and 5b). (Fig. 5a) represents a faulty R-element in conductive causality modeled by BG-LFT, where the modulated source $MSf : w_R$ represents the flow generated by the multiplicative fault, $Df^* : Z_R$ is a fictive sensor, and R is the nominal parameter.

Fig. 5b shows a subsystem containing a faulty R-element in conductive causality and a detector SSe modeled by BG-LFT. From the 0-junction connected to the detector SSe , the following ARR can be generated:

$$ARR = f_{SSe} + f_1 - f' = 0; \quad f_{SSe} = 0;$$

$$ARR = f_1 - \left(\frac{1}{R}\right)e_{SSe} - \left(\frac{1}{R}F_{1/R}\right)e_{SSe} = 0; \quad (6)$$

Where the inactive variable f_{SSe} is equal to zero. This means that the inactive variable of a flow and effort detector is the effort the flow and, respectively. Without the presence of the fault, the residual is given by

$$r = f_1 - \left(\frac{1}{R}\right)e_{SSe} \quad (7)$$

In the presence of the fault, the residual is equal to:

$$\left(\frac{1}{R}F_{1/R}\right)e_{SSe} \quad (8)$$

Thus, if the fault is null the residual is zero. In addition, the residual is equal to the inactive variable of the detector f_{SSe} .

This means that the residual is represented in the BG model by the inactive variable of the associated detector. Therefore, it is possible to generate the sensitivity relation between the residual and the fault from the BG model. This can be done by using Mason's rule [19].

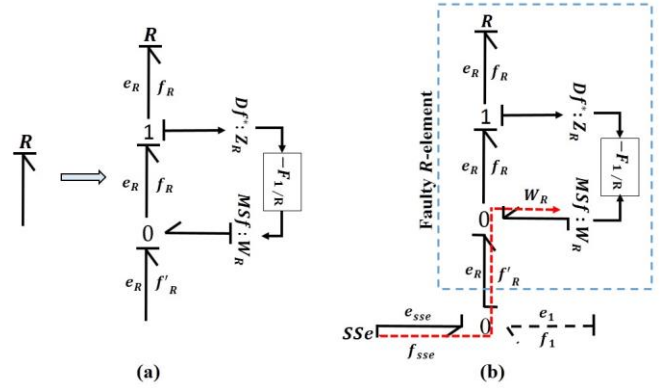


Fig. 5. (a) Faulty R-element in conductive causality, and (b) Bi-causal faulty R-element.

V. APPLICATION

In this section, the fault diagnosis performance and capability of each method previously described are compared by applying them to an electrical system (Fig. 6a). The obtained FSM by each method is analyzed in order to conclude about fault isolability capability. The system is composed of two capacitance elements ($C : C_1$ and $C : C_2$), a resistance element ($R : R_1$), a transformer element ($TF : 1/N$), and the source of flow that represented by the current input $Sf : I_0$. The system is equipped with two voltage sensors represented in the model by $De : e_{m1}$ and $De : e_{m2}$. The BG model in derivative causality of this electrical system is illustrated in Fig. 6b, where the derivative causality is assigned to it, and the detectors are replaced by signal sources of effort ($SSe : e_{m1}$ and $SSe : e_{m2}$).

The considered system contains two sensors connecting to two junctions (O_1 and O_2). Thus, according to the causality inversion method (see section 2), two ARR s can be generated:

$$ARR_1 = I_0 - C_1 \frac{e_{m1}}{dt} - \frac{e_{m1} - \frac{1}{N}e_{m2}}{R_1} \quad (9)$$

$$ARR_2 = \frac{e_{m1} - \frac{1}{N}e_{m2}}{NR_1} - C_2 \frac{e_{m2}}{dt} \quad (10)$$

Hence, the evaluation of these ARR s gives two residuals r_1 , and r_2 . By considering that faults may affect all system components, the following fault signature matrix represented in Table 2, can be obtained from (9, 10). We remark that all system components are detectable (Db),

however, the capacitance element $C : C_2$ is the only fault that can be isolated.

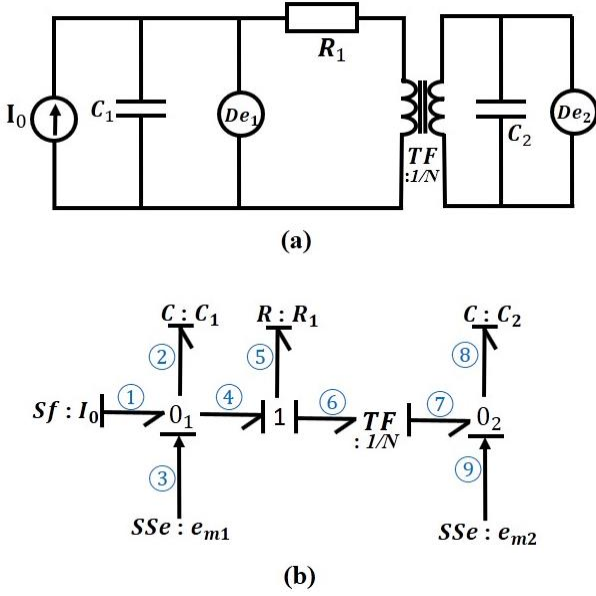


Fig. 6. (a) Schematic model of the electrical system, and (b) BG model of the electrical system in derivative causality.

TABLE II. THE FSM OBTAINED BY THE CAUSALITY INVERSION METHOD

Faults/residuals	r_1	r_2	Db	Ib
$De : e_{m1}$	1	1	1	0
$De : e_{m2}$	1	1	1	0
$Sf : I_0$	1	0	1	0
$C : C_1$	1	0	1	0
$R : R_1$	1	1	1	0
$TF : 1/N$	1	1	1	0
$C : C_2$	0	1	1	1

Consider that, at a time, only one of the existing detectors is used for diagnosis, where only $De : e_{m2}$ is used for diagnosis. Then the bi-causality is propagated from the double source ($SeSf : e_{m2}$) to $DeDf^* : e_{m1}^{\wedge}$, as depicted in Fig. 7a. The system remains observable and over-constrained, and since the sensor $De : e_{m1}$ is not isolable (Table 2), it is possible to compute an additional non-redundant ARR_3 without using $De : e_{m1}$ for diagnosis. In addition, the following constraint can be generated:

$$e_{m1}^{\wedge} = \frac{1}{N} e_{m2} + R_1 N C_2 \frac{de_{m2}}{dt} \quad (11)$$

Finally, in order to obtain ARR_3 (12), e_{m1} is replaced by e_{m1}^{\wedge} in ARR_3 .

$$ARR_3 : I_0 - C_1 \frac{e_{m1}^{\wedge}}{dt} - \frac{e_{m1}^{\wedge} - \frac{1}{N} e_{m2}}{R_1} = 0. \quad (12)$$

Following the same procedure while using only the information from the signal source $SSe : e_{m1}$ and ignoring the one of $SSe : e_{m2}$ (Fig. 7b). In addition, the following constraint can be obtained:

$$e_{m2}^{\wedge} = N \left(e_{m1} - R_1 \left(I_0 - C_1 \frac{de_{m1}}{dt} \right) \right). \quad (13)$$

Finally, in order to obtain ARR_4 (14), e_{m2} is replaced by e_{m2}^{\wedge} in ARR_4 .

$$ARR_4 : \frac{e_{m1} - \frac{1}{N} e_{m2}^{\wedge}}{NR_1} - C_2 \frac{de_{m2}^{\wedge}}{dt} = 0. \quad (14)$$

These four ARR are used to compute a new FSM, illustrated in Table 3. We Remark that all the system components are detectable and the set of isolable faults is the following: $[C : C_2, De : e_{m1}, De : e_{m2}]$ Therefore, with this method, two new faults are isolable.

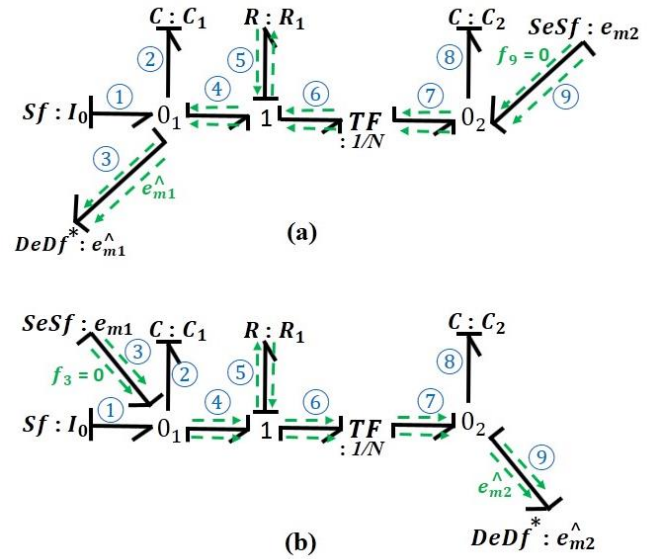


Fig. 7. (a) BG model of the system in bi-causality for e_{m1}^{\wedge} estimation, and (b) BG model of the system in bi-causality for e_{m2}^{\wedge} estimation.

TABLE III. FSM OF THE SYSTEM OBTAINED BY AUGMENTED ARRS

Faults/residuals	r_1	r_2	r_3	r_4	Db	Ib
$De : e_{m1}$	1	1	0	1	1	1
$De : e_{m2}$	1	1	1	0	1	1
$Sf : I_0$	1	0	1	1	1	0
$C : C_1$	1	0	1	1	1	0
$R : R_1$	1	1	1	1	1	0
$TF : 1/N$	1	1	1	1	1	0
$C : C_2$	0	1	1	1	1	1

According to the fault signature matrix (Table 2), four faults ($R:R_1, De:e_{m1}, De:e_{m2}, TF:1/N$) have the same signature $\{11\}$, and two residuals (r_1 and r_2) are sensitive to them. So, these four faults can be isolated using the fault estimation equations (see section 4).

Let us now consider a fault affecting the parameter element $R:R_1$. It is estimated from two ways by using the residuals r_1 and r_2 . The two estimation equations of $R:R_1$ parameter fault from r_1 (Fig. 8a) and from r_2 (Fig. 8b) can be obtained:

$$\begin{cases} F_{1/R_1}^1 = \frac{1}{R_1} \left(e_{m1} - \frac{1}{N} e_{m2} \right) r_1 \\ F_{1/R_1}^2 = \frac{-N}{R_1} \left(e_{m1} - \frac{1}{N} e_{m2} \right) r_2 \end{cases} \rightarrow r_3 = F_{1/R_1}^1 - F_{1/R_1}^2 \quad (15)$$

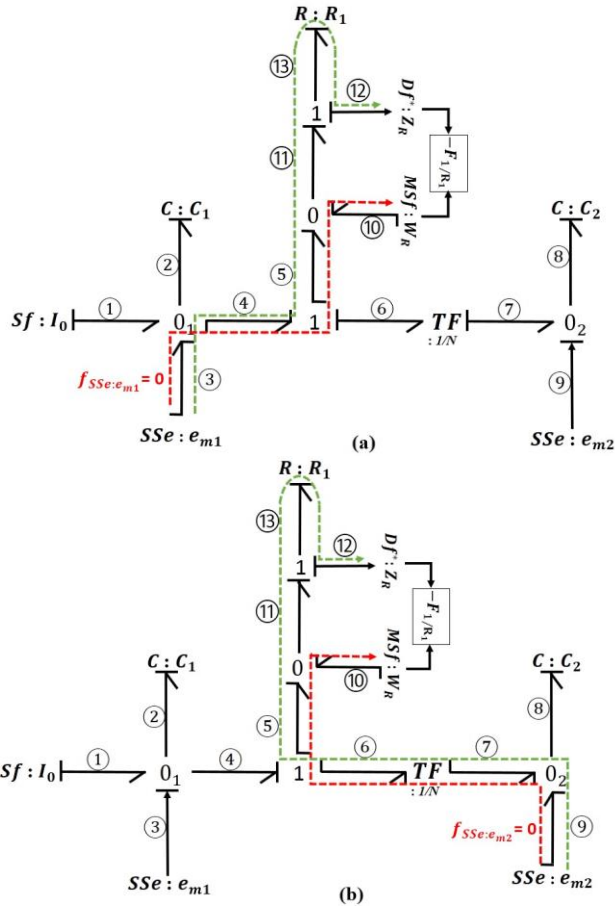


Fig. 8. (a,b) Fault estimation of $R:R_1$ parameter fault using r_1 and r_2 .

We notice that the residual r_3 is not sensible to the faults that affect the $R:R_1$ parameter component because F_{1/R_1}^1 and F_{1/R_1}^2 are the estimations of this fault. Following the

same procedure, we can obtain the estimation equations of $De:e_{m1}, De:e_{m2}$, and $TF:1/N$. Where r_4, r_5 and r_6 are the residuals generated from the comparison of the two estimation equations of each fault respectively. Finally, by considering these new residuals, the fault signature matrix illustrated in Table 4 is obtained. It can be noticed that this method clearly increase the number of isolable faults of the system. In this case, five system components can be isolated. Therefore, with this method, two new faults can be isolated compared with the two methods described previously.

TABLE IV. FSM WHEN THE FAULT ESTIMATION PERFORMED

Faults/residuals	r_1	r_2	r_3	r_4	r_5	r_6	Db	Ib
$De:e_{m1}$	1	1	1	0	1	1	1	1
$De:e_{m2}$	1	1	1	1	0	1	1	1
$Sf:I_0$	1	0	-	-	-	-	1	0
$C:C_1$	1	0	-	-	-	-	1	0
$R:R_1$	1	1	0	0	1	1	1	1
$TF:1/N$	1	1	1	1	1	0	1	1
$C:C_2$	0	1	-	-	-	-	1	1

A. Simulation Results

To verify the efficiency of each method, an application using simulation data has been done. The input and output signals of the electrical system are depicted in Fig. 9. The four ARR_s 9, 10, 12, 14 are obtained using the augmented ARR_s method were tasted in a normal situation, and the residuals are evaluated in real-time, as depicted in Fig. 10. As expected, the residuals (r_1, r_2, r_3 and r_4) are close to zero and do not exceed the thresholds (the red dashed lines). This means that the electrical system is healthy (fault-free case).

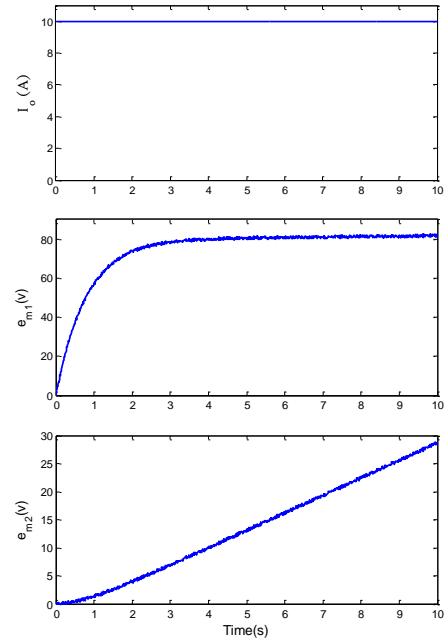


Fig. 9. The input and output signals of the system in normal functioning.

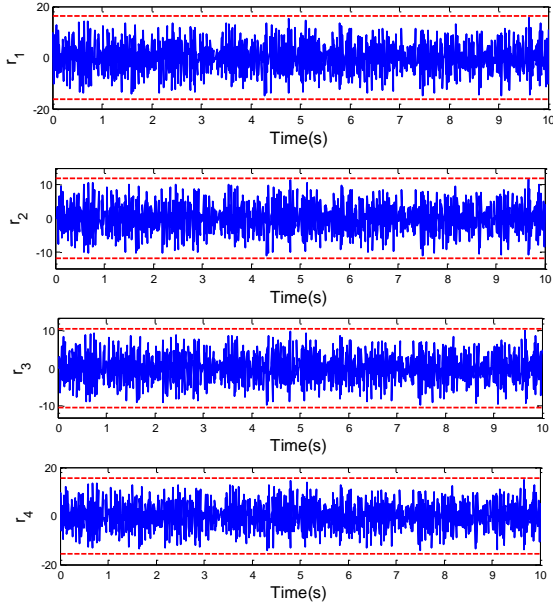


Fig. 10. r_1, r_2, r_3 and r_4 in normal functioning.

An additive fault is then introduced in the voltage sensor ($De: e_{m2}$) at time $t=5s$, which is not isolable by the causality inversion method. The signal of the faulty/healthy voltage sensor ($De: e_{m2}$) is illustrated in Fig. 11.

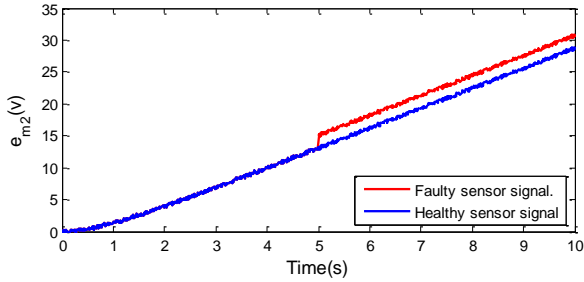


Fig. 11. The output of the faulty/healthy ($De: e_{m2}$) voltage sensor fault.

From the fault signature matrix (Table 3), the residuals sensitive to the introduced fault are r_1, r_2 , and r_3 . The residuals in case of the ($De: e_{m2}$) voltage sensor fault are illustrated in Fig. 12. As the structural results concluded, the residuals r_1, r_2 , and r_3 detect this fault and exceed the thresholds, while r_4 does not detect this fault because it is not sensitive to it. The signature $\{1110\}$, in this case, is the same as the signature of the $De: e_{m2}$ voltage sensor fault. It is then possible to conclude that a fault in the voltage sensor $De: e_{m2}$ can be isolated when the sensor data combinations method is performed.

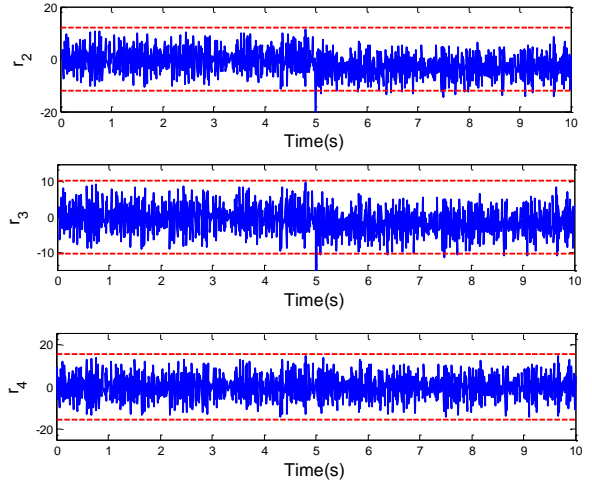
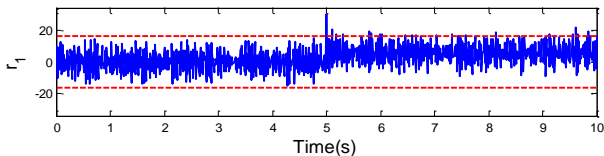
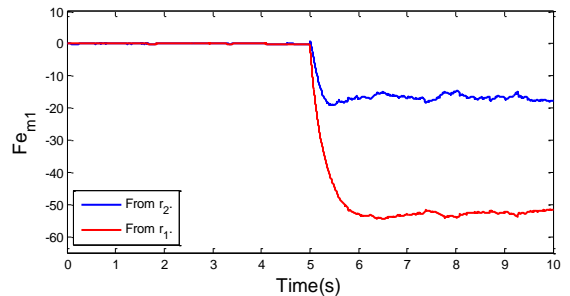
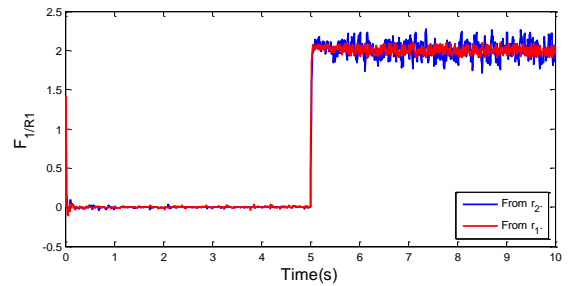


Fig. 12. r_1, r_2, r_3 and r_4 in case of ($De: e_{m2}$) voltage sensor fault.

Let us now consider another fault affecting the parameter element $R: R_1$. This fault is not isolable either by causality inversion method or by augmented ARR's method. According to the fault signature matrix (Table 4), this fault can be isolated using the fault estimation equations. This is verified by the simulations results shown in Fig. 13. The estimations of the faults are done after the detection of the fault (Fig. 14). This means that the estimation is off when the residual (r_1 and r_2) values are less than the threshold. The two estimations of F_{1/R_1} from r_1 , and r_2 are equal while the others are not (Fig. 13). This means that the residual r_3 is equal to 0, which is the comparison between the two estimations of the fault F_{1/R_1} from r_1 , and r_2 while r_4, r_5 and r_6 are equal to 1 because their estimations from r_1 , and r_2 are not equal. In this case, the fault on the $R: R_1$ parameter element is isolated.



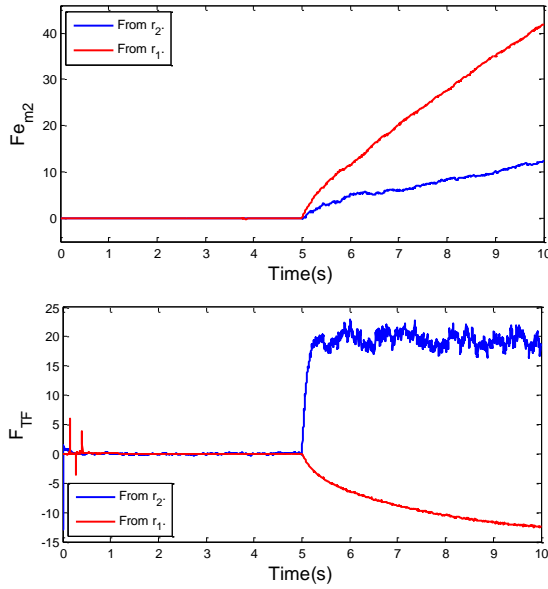


Fig. 13. F_{1/R_1} , $F_{e_{m1}}$, $F_{e_{m2}}$ and F_{TF} from r_1 and r_2 in case of $(R : R_1)$ fault.

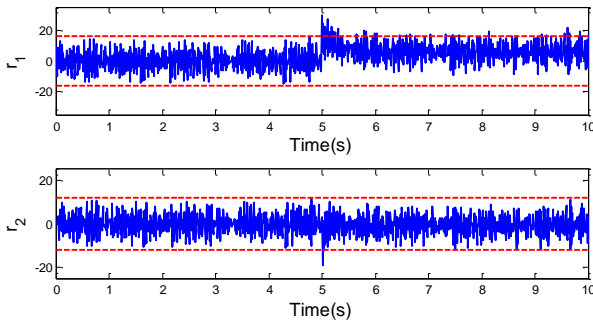


Fig. 14. r_1 and r_2 in case of $(R : R_1)$ fault.

B. Comparative Analysis

The advantages, drawbacks, and limitations of each method are summarized as follows:

1. Advantages:

1.1. Causality inversion method:

The *ARRs* are obtained in a systematic way using covering causal path methodology to eliminate the unknown variables. The diagnosis information is considered with less calculation.

1.2. Augmented *ARRs* method:

Can generate different versions of the same *ARR* without adding new sensors. Excellent capability for sensors fault isolation even if these faults has only one sensitive residual.

1.3. Fault estimation method:

Represent a simple and systematic way to obtain the fault estimation equations directly from the graphical model.

2. Drawbacks and limitations:

2.1. Causality inversion method:

Cannot isolate the faults that have the same signature (see Table 2). Does not exploit all possible sensor combinations.

2.2. Augmented *ARRs* method:

The system must remain over-constrained and observable when ignoring one of the sensors used for diagnosis, and this is not always available in all systems. A parameter fault can be isolated using this method if and only if its signature is different from all parameter and actuator faults (see Table 3).

2.3. Fault estimation method:

The generation of the sensitivity relations between the fault and the residual by using Mason's rule is only limited in the linear case and inverted non-linear systems.

VI. CONCLUSIONS

In this paper, a comparative study between three methods using bond graph approach and its causal and structural proprieties for fault diagnosis has been presented. The study indicates that both Augmented *ARRs* and fault estimation methods are the extension of the causality inversion method. The first method combines the sensor data in order to generate additional non-redundant *ARRs*. These additional *ARRs* enable to obtain the different set of fault signatures. The second is based on the sensitivity relations between the fault and the residual, in order to generate the fault estimation equations. These equations are used to improve the isolation of the faults have the same fault signature. Each of these methods has its own advantages and limitations. The results show that the fault estimation method can isolate more faults when compared to other methods.

REFERENCES

- [1] M. Thirumarimurugan, N. Bagyalakshmi, and P. Paarkavi, "Comparison of fault detection and isolation methods: A review," In Intelligent Systems and Control (ISCO), 2016 10th International Conference on. IEEE. pp. 1-6. January 2016.
- [2] Z. Zhu, Z. Ge, Z. Song, and L. Zhao, "Fault detection and identification: serial form versus simultaneous form," IFAC Proceedings Volumes. Vol.44, p. 2827-2832, 2011.
- [3] Y. Qian, L. Xu, X. Li, L. Lin, and A. Kraslawski, "LUBRES: An expert system development and implementation for real-time fault diagnosis of a lubricating oil refining process" Expert Systems with Applications. Vol. 35, p. 1252-1266, 2008.
- [4] S. Ding, P. Zhang, E. Ding, A. Naik, P. Deng, and W. Gui, "On the application of PCA technique to fault diagnosis" Tsinghua Science and Technology. Vol. 15, p. 138-144, 2010.
- [5] F. Pierri, G. Paviglianiti, F. Caccavale, and M. Mattei, "Observer-based sensor fault detection and isolation for chemical batch reactors," Engineering Applications of Artificial Intelligence, Vol. 21, p. 1204-1216, 2008.
- [6] M. Du, and P. Mhaskar, "Isolation and handling of sensor faults in nonlinear systems," Automatica. Vol. 50, p. 1066-1074, 2014.
- [7] S. X. Ding, "Model-based fault diagnosis techniques: design schemes, algorithms, and tools," Springer Science and Business Media. 2008.
- [8] H. M. Odendaal and T. Jones "Actuator fault detection and isolation: An optimized parity space approach," Control Engineering Practice. Vol. 26 222-232, 2014.
- [9] B. O. Bouamama, A. K. Samantaray, K. Medjaher, M. Staroswiecki and G. Dauphin-Tanguy, "Model builder using functional and bond graph

- tools for FDI design” *Control Engineering Practice*. Vol. 13, p. 875-891, 2005.
- [10] A. K. Samantaray and S. K. Ghoshal, “Bicausal bond graphs for supervision: From fault detection and isolation to fault accommodation,” *Journal of the Franklin Institute*. Vol. 345, 1-28, 2008.
- [11] W. Borutzky, “Bond graphs for modelling, control and fault diagnosis of engineering systems,” Springer. London, 2017.
- [12] B. O. Bouamama, A. K. Samantaray, K. Medjaher, M. Staroswiecki and G. Dauphin-Tanguy, “Derivation of constraint relations from bond graph models for fault detection and isolation,” *Simulation Series*. Vol. 35, p. 104-109, 2003.
- [13] A. K. Samantaray and B. O. Bouamama, “Model-based process supervision: a bond graph approach,” Springer Science and Business Media, 2008.
- [14] A. Termeche, D. Benazzouz, B. O. Bouamama, and I. Abdallah, “Augmented analytical redundancy relations to improve the fault isolation” *Mechatronics*. Vol. 55, p. 129-140, 2018.
- [15] P. J. Gawthrop, “Bicausal bond graphs,” *SIMULATION SERIES*. Vol. 27, p. 83-83. 1994.
- [16] Y. Touati, R. Merzouki, and B. O. Bouamama, “Fault estimation and isolation using bond graph approach,” *SAFEPROCESS-IFAC Mexico city, Mexico*. 2012.
- [17] Y. Touati, R. Merzouki, B. O. Bouamama, and R. Loureiro, “Detectability and Isolability Conditions in Presence of Measurement and Parameter Uncertainties Using Bond Graph Approach,” *SAFEPROCESS-IFAC, Mexico city, Mexico*. 2012.
- [18] C. S. Kam, G. Dauphin-Tanguy, “Bond graph models of structured parameter uncertainties,” *Journal of the Franklin Institute*. Vol. 342, p. 379-399, 2005.
- [19] F. T. Brown, “Direct application of the loop rule to bond graphs,” *Journal of Dynamic Systems, Measurement, and Control*, Vol. 94, p. 253-261. 1972.